Albumin adsorption on Cibacron Blue F3G-A immobilized onto oligo(ethylene glycol)-terminated self-assembled monolayers

Mª CRISTINA L. MARTINS[1,2]*, ESMAEEL NAEEMI[3], BUDDY D. RATNER[3], MÁRIO A. BARBOSA[1,2]
[1]*INEB – Instituto de Engenharia Biomédica, Laboratório de Biomateriais, Rua do Campo Alegre, 823, 4150-180 Porto, Portugal*
E-mail: cmartins@ibmc.up.pt
[2]*Universidade do Porto, Faculdade de Engenharia, Departamento de Engenharia Metalúrgica e Materiais, Porto, Portugal*
[3]*Department of Bioengineering and Department of Chemical Engineering, University of Washington, Seattle, WA 98195, USA*

Self-assembled monolayers can be tailored with specific ligands to a certain protein and at the same time prevent the non-specific adsorption of other proteins. Cibacron Blue F3G-A (CB-thiol) was successfully immobilized onto tetra(ethylene glycol)-terminated alkanethiol (CB-thiol). The affinity of human serum albumin (HSA) to immobilized Cibacron Blue F3G-A was studied using mixed thiolate self-assembled monolayers on gold with different *n*-alkyl chain lengths and functional terminal groups (CH_3-; OH- and tetra(ethylene glycol)).

Surfaces were characterized using X-ray photoelectron spectroscopy and water contact angle measurements. Albumin adsorption and exchangeability of the adsorbed albumin molecules with other albumin molecules in solution were evaluated using ^{125}I-radiolabeled HSA. Competitive adsorption between albumin and fibrinogen to the different self-assembled monolayers (SAMs) was also investigated. Results showed that the incorporation of CB-thiol on the monolayers does not increase the HSA adsorption and reversibility on the SAMs. However, although specific adsorption of HSA to the immobilized Cibacron Blue F3G-A was not demonstrated, the presence of CB-thiol decreases the affinity of fibrinogen to the OH-terminated SAMs.

1. Introduction

Engineered surfaces optimized to bind specific proteins important for blood compatibility and biocompatibility have been described as a pathway for the development of new biomaterials [1]. Since albumin-coated surfaces have, in many experiments, been found to reduce platelet reaction to synthetic materials [2–4], research has been conducted to create surfaces that attract and bind albumin from the bloodstream, in a selective way. This involves the immobilization of ligands (e.g., alkyl chains of 16 and 18 carbon residues [5, 6], Cibacron Blue F3G-A [7, 8] or warfarin [9]) or antibodies to albumin [10, 11], at the surface of the biomaterial.

The ligand Cibacron Blue F3G-A is a monochlorotriazine dye (Fig. 1), which contains three acidic sulfonate groups and four basic primary and secondary amino groups [12]. This dye, after immobilization onto appropriate insoluble supports, has been used as a ligand in affinity chromatography to isolate and remove albumin from human plasma [13]. Although, the exact mechanism of the HSA binding to Cibacron Blue is still unclear, it was proposed that bilirubin-binding sites of albumin are significant in the interaction [14].

Keogh and Eaton [7] demonstrated that Cibacron Blue F3G-A bound to dextran and immobilized onto a polyetherurethane surface via an acrylamide link, binds albumin from human plasma in a selective and reversible way. Wang *et al*. [8] showed that polyurethanes modified by a poly(ethylene oxide) coupling-polymer with Cibacron Blue F3G-A endgroups, present a high capacity to bind albumin selectively from binary mixtures of albumin/fibrinogen. This selectivity was dependent of the length of the poly(ethylene oxide) spacer.

Recently, it was reported that Cibacron Blue F3G-A bound to poly(hydroxyethyl methacrylate) graft polymerized onto polyetherurethane (PU-PHEMA) increases albumin adsorption but also increases the adsorption of fibrinogen, thus showing low selectivity to albumin [15].

*Author to whom all correspondence should be addressed.

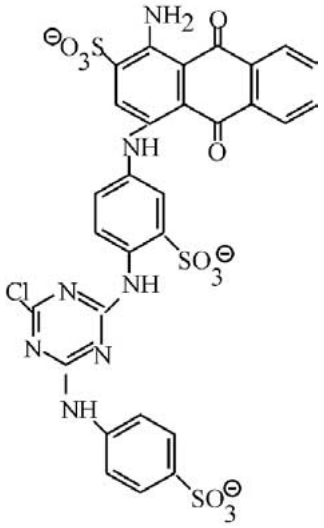

Figure 1 Chemical structure of Cibacron Blue F3G-A.

Since human serum albumin (HSA) carries specific binding pockets for Cibacron Blue [14, 16], and in solution Cibacron Blue binds only to HSA and not to fibrinogen [15], it was suggested that the lack of selectivity of these surfaces to albumin could be related to the fact that Cibacron Blue was not favorably exposed on the surface, in order to be recognized by the binding sites of HSA. Another explanation attributes the lack of specificity to the support, that may not adequately resist the non-specific adsorption of other proteins.

In order to clarify the affinity of surface-immobilized Cibacron Blue to albumin, this dye must be immobilized on well-defined surfaces. Self-assembled monolayers (SAMs) of alkanethiolates on gold represent a class of substrates that can precisely control the structure, density and pattern of immobilized ligands [17]. SAMs can be easily prepared by immersing a clean film of gold into a solution of terminally substituted alkanethiols $HS(CH_2)_nR$. The sulfur moiety of the alkanethiol binds strongly to gold, immobilizing the tail of the molecules to the surface. The intermolecular forces between the methylene chains and limited sulfur molecular mobility in the plane of the gold surface allow the molecules to pack tightly in an orientation nearly perpendicular to the surface of the gold film, orienting outward their terminal (head group) functionality (R) [18–20].

For the preparation of surfaces with specificity to a certain protein, non-specific interactions should be inhibited. Surfaces that resist the adsorption of proteins may serve this purpose. SAMs prepared from alkanethiols terminated in short ethylene glycol oligomers ($HS(CH_2)_{11}(OCH_2CH_2)_nOH$ with $n = 2$–7) are resistant to protein adsorption [21–24] and can be easily derivatized through its hydroxyl terminal group.

In the present study, tetra(ethyleneglycol)-undecanethiols (EG-thiol) were synthesized and derivatized with Cibacron Blue F3G-A (CB-thiol). SAMs were prepared using this CB-thiol mixed with EG-, OH- or CH_3-thiols (Table I shows the name, chemical formula and the abbreviation of the thiols used). Mixed SAMs were used in order to expose and dilute the Cibacron Blue molecules on the surface of the monolayer to allow optimal fitting of this ligand into HSA pockets. Three different model systems were produced (Fig. 2). On EG–CB mixed SAMs, CB-thiol was mixed with a non-fouling thiol (EG-thiol). Cibacron Blue was not expected to protrude from the non-fouling background. On OH–CB and CH_3–CB mixed SAMs, CB-thiol was mixed with a hydrophilic thiol (OH-thiol) and a hydrophobic thiol (CH_3-thiol), respectively. In these two SAMs, the Cibacron Blue molecule protrudes from the hydrophilic and hydrophobic background by a hydrophilic spacer. Surfaces were characterized using X-ray photoelectron spectroscopy (XPS) and water contact angle measurements. Albumin adsorption and exchangeability of the adsorbed albumin molecules with other albumin molecules in solution were evaluated using ^{125}I-radiolabeled HSA. Competitive adsorption between albumin and fibrinogen to the different SAMs was also investigated. Fibrinogen was used as a competitive protein because it is known to adsorb readily to implant surfaces and to be associated with potentially adverse host responses, such as coagulation and platelet adhesion and aggregation [25].

2. Material and methods

2.1. Gold substrates

Gold substrates for XPS and contact angle measurements were prepared using an automated, load locked ion beam deposition system (Nordiko N3000). Details on the machine can be found elsewhere [26]. The chromium (5 nm) and gold (25 nm) films were deposited by ion beam sputtering from gold and chromium targets (99.9% purity), respectively, onto silicon wafers (polished/etched, crystal orientation ⟨1 0 0⟩, from AUREL Gmbh). The thin layer of chromium was used to improve adhesion of gold to silicon. Deposition rates are 0.050 nm/s for chromium and 0.033 nm/s for gold. Deposition pressure was 3.5×10^{-5} Torr. The wafers were diced into pieces (1×1 cm^2) using a DISCO DAD 321 automated saw. Before dicing, all wafers were coated with 1.5 μm of photoresist (reference PFR7790EG, from JSR Electronics), which is soluble in acetone, to protect the film surface.

TABLE I List of alkenothiols used for self-assembled monolayers formation on the gold surfaces

Name of alkyl thiol	Chemical formula	Abbr.
11-mercapto-1-undecanol	$HS(CH_2)_{11}OH$	OH-thiol
1-hexadecanethiol	$HS(CH_2)_{15}CH_3$	CH_3-thiol
1-[mercaptoundec-11-yl]-tetra(ethylene glycol)	$HS(CH_2)_{11}(OCH_2CH_2)_4OH$	EG-thiol
1-[mercaptoundec-11-yl]-tetra(ethylene glycol) bonded to Cibacron Blue F3G-A	$HS(CH_2)_{11}(OCH_2CH_2)_4O$–Cibacron Blue F3G-A	CB-thiol

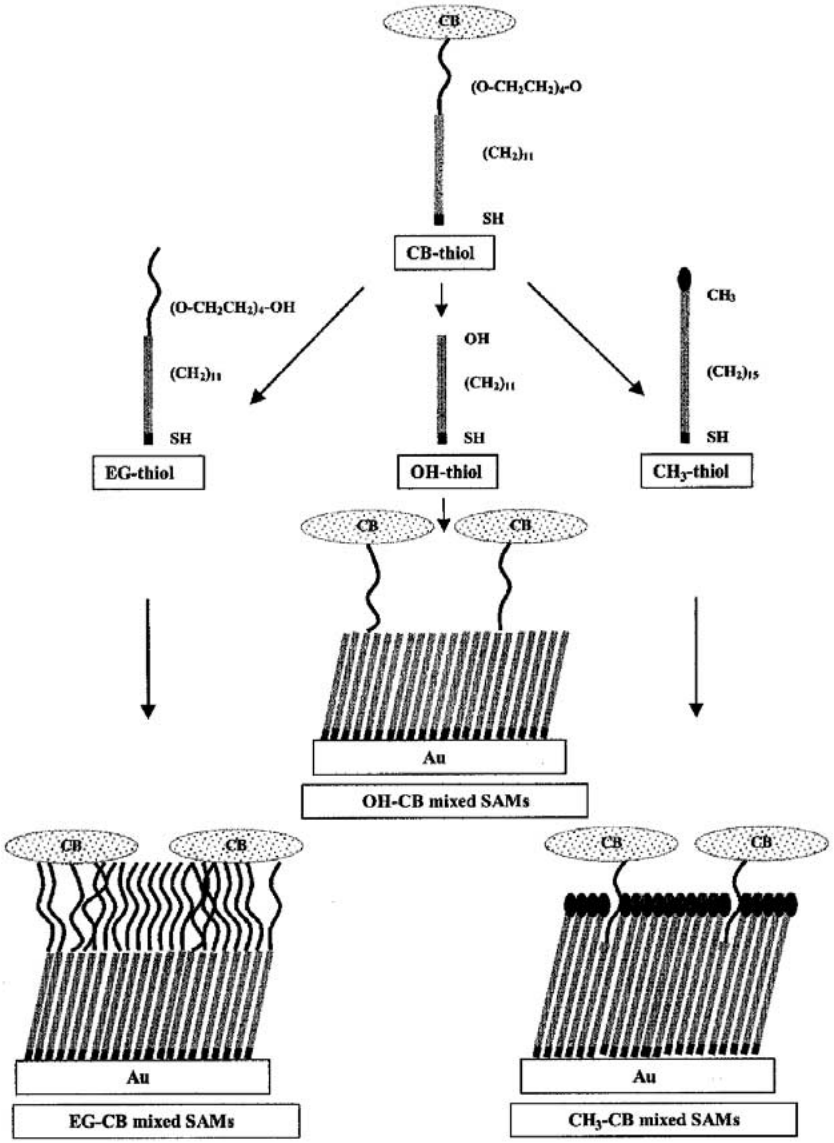

Figure 2 Idealized models for mixed self-assembled monolayers (SAMs) on gold prepared from ethanolic mixtures of CB-thiol with EG-, OH- and CH_3-thiols.

2.2. Synthesis of thiols

The following chemicals were used as received without further purification. Tetraethylene glycol (Aldrich 99%), undec-10-enyl bromide (Lancaster 97%), silica gel (Aldrich 230–400 mesh, 60 A), thiolacetic acid (Aldrich 96%), 1,1′-azobis(cyclohexanecarbonitrile) (Aldrich 98%) and Cibacron Blue F3G-A (Aldrich, Reactive Blue 2, dye content $\sim$ 60%)

The synthesis of the EG- [27] and CB-thiols is illustrated in Fig. 3.

2.2.1. Syntheses of undec-1-en-11yl-tetra(ethylene glycol) (I)

A mixture of 50% aqueous sodium hydroxide (21 mmol, 1.68 ml) and tetraethylene glycol (10 mmol, 1.94 g) was stirred for about 1 h in an oil bath at 100 °C under an atmosphere of nitrogen. To the above mixture undec-10-enyl bromide (21 mmol, 4.89 g) was added and the reaction continued. After 16 h the reaction mixture was cooled and extracted six times with hexane. Removal of hexane under reduced pressure gave a yellow oil. This oil was purified by column chromatography on silica gel (eluent: ethyl acetate) and gave 2.58 g of the product in 75% yield.

2.2.2. Synthesis of [1- [(methylcarbonyl)thio]undec-11-yl]tetra(ethylene glycol) (II)

A solution of I (5 mmol, 1.73 g) in methanol (15 ml) and thiolacetic acid (20 mmol, 1.52 g) and radical initiator 1,1′-azobis(cyclohexanecarbonitrile) (5 mg) were irradiated for 10 h under nitrogen with a 450 W medium-pressure mercury lamp. The mixture was concentrated in a rotary evaporator at reduced pressure to give 1.7 g of product in 81% yield.

2.2.3. Synthesis of (1-mercaptoundec-11-yl)tetra(ethylene glycol) (EG-thiol) (III)

Compund II (3.5 mmol, 1.5 g) was added to 50 ml solutions of 0.1 M HCL in methanol. The mixture was refluxed under an atmosphere of nitrogen for 6 h. The reaction mixture was concentrated by rotary evaporation at reduced pressure followed by purification of the

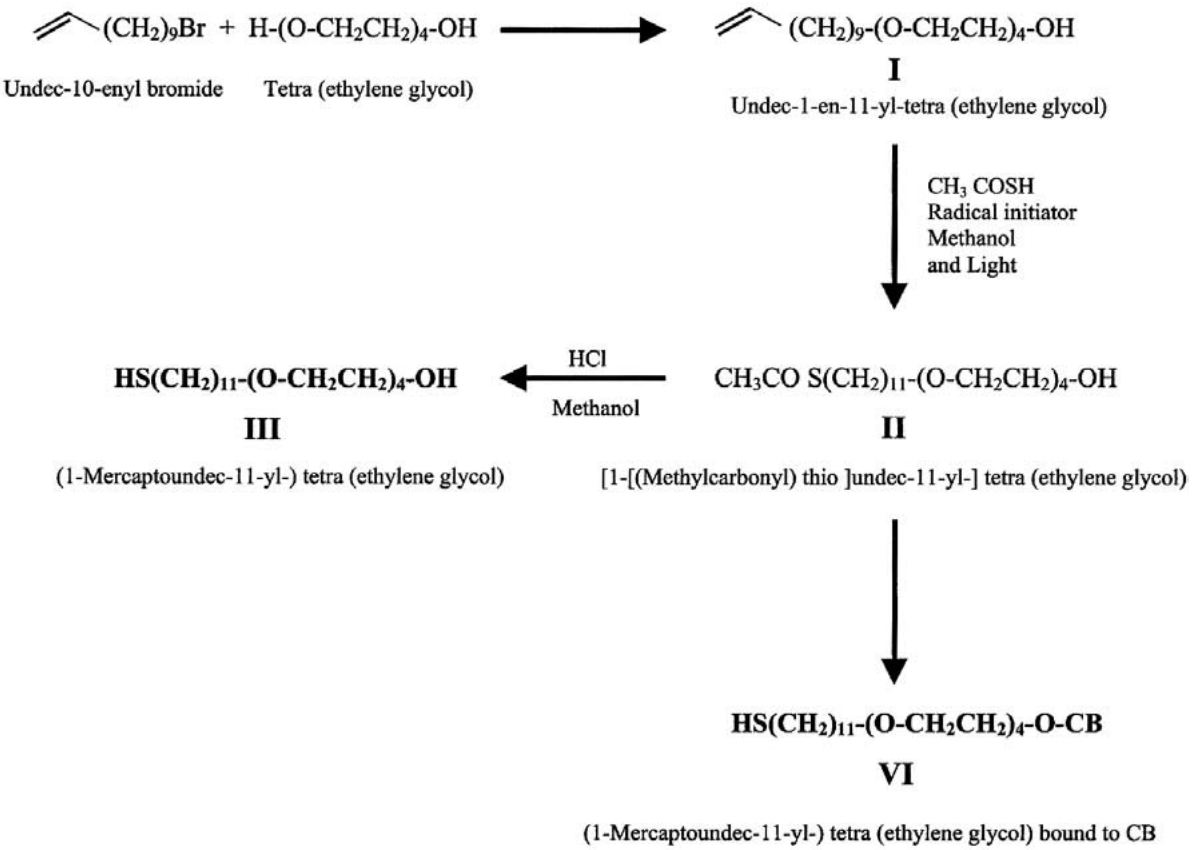

Figure 3 Synthesis procedure for tetra(ethyleneglycol)-undecanethiol (III) and Cibacron Blue F3G-A bound to tetra(ethyleneglycol)-undecanethiol (IV).

residues by chromatography on preparative TLC plates C18-silica gel and acetonitrile as the mobile phase gave 910 mg of product, a 68% yield.

2.2.4. Synthesis of EG-thiol bonded to CB-thiol (IV)

To a solution of compound II (1.1 mmol, 0.5 g) in ethanol (30 ml), a solution of Cibacron Blue F3G-A (1.1 mmol, 1.5 g) in BO_3H_3:NaOH buffer pH 9.8 (100 ml) was added. The reaction mixture was heated under nitrogen at 80 °C. After 8 h, the pH of the solution was raised to 13.0 with 6 M NaOH and the reaction continued at 80 °C for an additional hour. The reaction mixture was cooled to room temperature and was neutralized with a 1 M solution of HCl. Solvent was removed under reduced pressure. The crude product was extracted six times with cold methanol (20 ml each). The methanol was removed under reduced pressure to obtain the final product in 90% yield.

2.3. Monolayer formation

11-mercapto-1-undecanol ($SH-(CH_2)_{11}OH$; 97%, Aldrich) and 1-hexadecanethiol ($SH-(CH_2)_{15}CH_3$; 92%, Aldrich) were used as received. Thiol solutions were prepared in ethanol (Merck, 99.8%) with a final concentration of 1 mM. Mixed SAMs were obtained by mixing the pure thiol solutions in different percentages (Table II). All the solutions were prepared in a nitrogen environment inside a glove box. Just before use, gold substrates were cleaned twice in acetone and immersed in a ''piranha'' solution (7 parts concentrated H_2SO_4 and 3 parts 30% H_2O_2) for 10 min. (*Caution: this solution reacts violently with many organic materials and should be handled with great care.*) Substrates were rinsed sequentially with ethanol, water (distilled and deionized) and ethanol for 2 min in an ultrasonic bath. After being blown dry with a stream of argon, gold slides were immersed in the alkanethiol solutions. Incubation was performed at room temperature over 24 h in a nitrogen environment. After incubation, the monolayers were washed three times in fresh ethanol in an ultrasonic bath for 2 min. Monolayers were blown dry with a stream of argon and maintained in a container filled with nitrogen until used.

TABLE II Percentages of the different alkanethiols used in ethanolic solutions for the formation of self-assembled monolayers on the gold surfaces

SAMs	Alkanethiols (%)			
	CB-thiol	EG-thiol	OH-thiol	CH_3-thiol
EG	—	100	—	—
OH	—	—	100	—
CH_3	—	—	—	100
CB	100	—	—	—
EG–CB	80	20	—	—
OH–CB	80	—	20	—
CH_3–CB	80	—	—	20

2.4. XPS characterization

XPS measurements were carried out on a VG Scientific ESCALAB 200A (UK) spectrometer using magnesium Kα (1253.6 eV) as a radiation source. The photoelectrons

were analyzed at take off angles of 90° and 55°. Survey spectra were collected over a range of 0–1150 eV with an analyzer pass energy of 50 eV. High-resolution C(1s), O(1s), N(1s), S(2p) and Au(4f) spectra were collected with an analyzer pass energy of 20 eV. The binding energy (BE) scales were referenced by setting the $Au_{4f7/2}$ BE to 84.0 eV. All the spectra were fitted using an XPS peak fitting program (XPSPEAK Version 4.1). All the carbon spectra were fitted using asymmetrical 70% Gaussian/30% Lorentzian profiles.

Sulfur high resolution spectra were fitted with a doublet structure centered at 162 and 163.2 eV and a peak area ratio of 2 : 1 as described by Castner *et al*. [28] for the thiolates on gold. The sulfur spectra with higher binding energy were also fitted with a doublet structure centerd at 168 and 169.2 eV and a peak area ratio of 2 : 1 [29].

2.5. Contact angle measurements

Contact angle measurements were performed using the sessile drop method with a contact angle measuring system from Data Physics, model OCA 15, equipped with a video CCD-camera and SCA 20 software. The equipment incorporates an electronic syringe unit with a gas-tight 500 µl dosing syringe (Hamilton). SAMs ($1 \times 1\,cm^2$) were placed in a closed, thermostated chamber (25 °C), saturated with the liquid sample in order to prevent evaporation of the liquid from the drop. After deposition of 4 µl drops of distilled and deionized water, images were taken every 2 s over 600 s. Time-dependent contact angles were determined using the SCA 20 software (Data Physics). The water contact angle for each SAM was calculated by extrapolating the time-dependent curve to zero. Four replicates were used.

2.6. Protein solutions

Protein solutions were obtained by dissolving HSA (Sigma, ref. A1653) or human fibrinogen (HFG; Sigma, ref. F4129) in PBS (Sigma, pH 7.4, lot 109H8205) with 0.01 M NaI–iodinated PBS. The final concentration of the protein solutions was 0.1 mg/ml.

2.7. Quantification of adsorbed albumin

Quantification of adsorbed HSA on the different monolayers was performed using ^{125}I-labeled HSA. HSA was labeled using the iodo-gen method [30, 31]. Purification of the labeled protein was performed using Sephadex G-25 M columns (PD-10: Amersham pharmacia biotech). HSA iodination reaction yield was 90% determined by precipitating the ^{125}I-labeled protein with 20% trichloro acetic acid (TCA: Merck). ^{125}I-labeled protein was added to unlabeled protein solution in order to obtained a final activity of 6×10^8 cpm/mg.

For the HSA adsorption measurements, all the SAMs were placed in a 24-well tissue culture plate (Sarsted) with the surface facing up and a drop of 7 µl of HSA solution was pipetted onto each SAM. Iodinated buffer (PBSI) was used in order to prevent adsorption of some free iodine [32, 33]. A small amount of PBSI was added to the periphery of the wells to maintain a moist environment. Adsorption tests were carried out at 25 °C for 1 h. After protein adsorption, each well was rinsed four times with 2 ml of PBS. The activities were counted with the samples placed in radio-immunoassay tubes. Three replicates were used. The counts of each sample were averaged and the surface concentration was calculated by the equation:

$$\mathrm{HSA(mg/m^2)} = \frac{\mathrm{Counts\ (cpm)}}{\mathrm{A_{solution}\ (cpm/mg)} * \mathrm{SA\ (m^2)}}$$

where the Counts are the radioactivity of the SAMs, $A_{solution}$ is the specific activity of the protein solution and SA is the area of contact of the drop with substrate. Except for the more hydrophobic CH_3-terminated SAMs and the gold sample, SA coincided with the total surface of the sample. For CH_3-terminated SAMs and gold, the SA was calculated using the drop contact diameter obtained using the contact angle measuring system software described before, for the same conditions used during the protein adsorption test.

Exchangeability tests were carried out by immersing the labeled SAMs in a unlabeled HSA pure solution (1 mg/ml, 24 h, 25 °C). The samples were then washed with the buffer and their residual radioactivity was counted.

For competitive adsorption of HSA in the presence of fibrinogen, the concentration of ^{125}I-HSA was 0.1 mg/ml and the quantity of non-labeled HFG was 0.1 mg/ml. The amount of HSA adsorbed from pure albumin solution was considered as 100% for all subsequent calculations.

3. Results

3.1. Synthesis of thiols

NMR and IR spectroscopy demonstrated that the compounds obtained by synthesis were EG-thiol and EG-thiol with a terminal Cibacron Blue F3G-A head group (CB-thiol) (data not shown).

3.2. Surface characterization of SAMs

3.2.1. XPS

All the SAMs were analyzed by XPS. This technique was used to verify the presence of Cibacron Blue, as well as to characterize the composition of the SAMs. The presence of nitrogen and sulfur in a higher oxidation state provides a marker for the presence of Cibacron Blue. Fig. 4 shows the XPS high-resolution spectra of the S(2p) region for SAMs with and without Cibacron Blue (CB- and EG-terminated SAMs respectively). All the monolayers exhibit a S(2p) peak at a binding energy centered at 162 eV that is characteristic of thiolates on gold [28]. SAMs with Cibacron Blue show an additional S(2p) peak at a binding energy of 168 eV. This peak is associated with sulfur bound to three oxygen atoms [29, 34–36], i.e., the sulphonate present in Cibacron Blue (Fig. 1).

The expected (calculated from the stoichiometry of the thiols used) and the observed (calculated from the XPS high-resolution spectra) atomic composition of all the SAMs are given in Table III. Survey spectra (data not

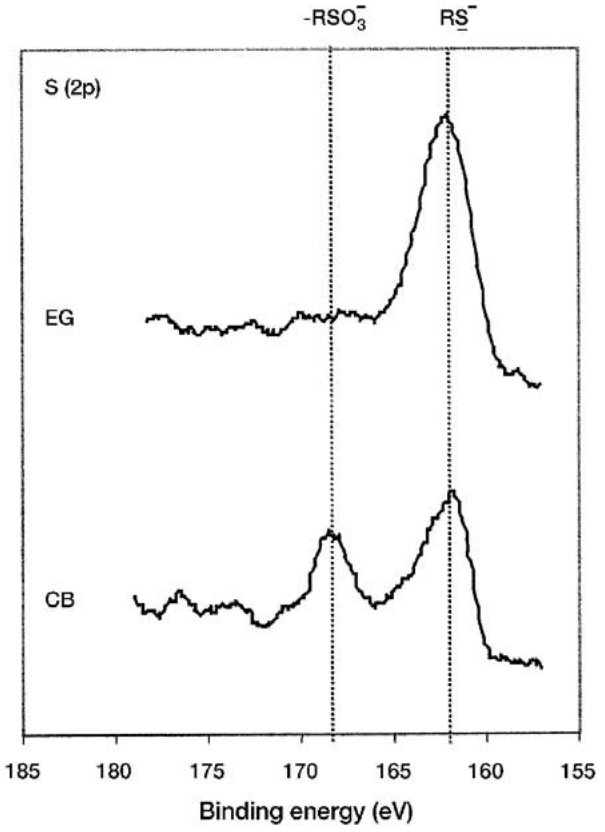

Figure 4 XPS high-resolution spectra of S(2p) region SAMs with and without Cibacron Blue F3G-A (CB- and EG-terminated SAMs respectively).

shown) reveal the presence of only the desired monolayer elements (Au, C, O, S and N), thus indicating the absence of contamination. Concerning EG-, OH- and CH_3-terminated SAMs, XPS results are similar to those described by other authors [19, 37]. For EG- and OH-terminated SAMs, the oxygen atomic percentage was higher than the theoretical value, where oxygen was situated on the outermost side of the monolayer [19]. The lower sulfur atomic percentage (162 eV) of the EG-, OH- and CH_3-terminated SAMs is usually attributed to the inelastic scattering of the S2p photoelectrons within the monolayer [19].

XPS data also show that nitrogen was only detected on SAMs prepared from CB-thiol solutions (CB; EG–CB; OH–CB and CH_3–CB). The mixed SAMs were prepared from mixtures of 80% CB-thiol with 20% of other thiols. SAMs using lower percentages of CB-thiols (60% and 40%) were also produced and analyzed by XPS. However, since no nitrogen was detected by XPS, these mixed SAMs were not subsequently used in this study. Except for CH_3–CB mixed SAMs, nitrogen and oxidized sulfur (168 eV) are found simultaneously, confirming the presence of Cibacron Blue on these surfaces. The detection of oxygen (1.9 at %) and nitrogen (0.6 at %) on CH_3–CB mixed SAMs also indicates the incorporation of CB-thiol on these monolayers. However, the low percentage of nitrogen, probably explains why oxidized sulfur was not detected (the atomic ratio of nitrogen to sulfur in CB is 7 : 3).

It was also observed that all the SAMs with Cibacron Blue showed lower atomic percentages of nitrogen and oxidized sulfur (168 eV) than the expected. For mixed SAMs, these results may suggest a strong preference for the adsorption of thiols without Cibacron Blue. However, for pure CB-terminated SAMs these results may suggest some disorder of the monolayer. The expected percentage of Cibacron Blue incorporation in mixed monolayers was calculated using the nitrogen atomic composition of these mixed-SAMs normalized to the nitrogen obtained from pure CB-terminated SAMs. The percentages of CB-thiol incorporation on EG–CB, OH–CB and CH_3–CB mixed SAMs are 75, 68 and 9, respectively. CH_3–CB mixed SAMs presented a very

TABLE III Surface atomic percentage of all the SAMs used, with and without Cibacron Blue F3G-A, calculated from the XPS high-resolution spectra (observed) and from the stoichiometry of the thiols used (expected)

SAMs	Atomic (%)				
	C (1s)	O (1s)	S1(2p) 162 eV	S2(2p) 168 eV	N (1s)
CB					
Observed	68.7	20.6	2.7	1.5	6.5
Expected	64.1	21.3	1.3	4.0	9.3
EG					
Observed	75.2	22.6	2.2	—	—
Expected	76.0	20.0	4.0	—	—
EG–CB					
Observed	67.3	22.3	4.3	1.1	4.9
Expected	66.5	21.0	1.9	3.2	7.4
OH					
Observed	82.4	13.5	4.1	—	—
Expected	84.6	7.7	7.7	—	—
OH–CB					
Observed	75.2	16.0	4.0	0.5	4.4
Expected	68.1	18.7	2.6	3.2	7.4
CH_3					
Observed	96.6	—	3.4	—	—
Expected	94.0	—	6.0	—	—
CH_3–CB					
Observed	94.3	1.9	3.2	—	0.6
Expected	70.1	17.1	2.2	3.2	7.4

TABLE IV Surface atomic percentage of CB-terminated SAMs calculated from the XPS high-resolution spectra. XPS analysis was performed using two different take-off angles (55 and 90°)

CB–SAM	Atomic (%)	
	55°	90°
C (1s)	55	39
O (1s)	17	10
S1 $(2p)_{162\,eV}$	2	3
S2 $(2p)_{168\,eV}$	1	1
N (1s)	5	4
Au (4f)	20	43
$S_{(168\,eV)}/S_{(162\,eV)}$	0.5	0.3

low CB-thiol incorporation, indicating a strong preference for the adsorption of the CH_3-thiol.

In order to find out if Cibacron Blue is localized on the surface of the monolayer, pure CB-terminated SAMs were analyzed using angle-dependent XPS. The take-off angles used were 55° and 90°. The take-off angle is described as the angle between the surface and the photoelectrons accepted by the analyzer. As the take-off angle decreases the surface sensitivity of XPS increases since the depth of analysis decreases. Table IV shows the atomic compositions of the CB-terminated SAM using the two different take-off angles. As expected, gold and sulfur (162 eV – from thiolate on gold) intensities increase and carbon and oxygen intensities decrease with the depth of the analysis. The atomic percentage of oxidized sulfur (168 eV) does not change with the depth of the analysis, probably because of statistical error due to low atomic percent. The fraction of nitrogen increases as the sampling depth decreases suggesting the presence of Cibacron Blue on the surface of the monolayer. The decrease of $S_{(168\,eV)}/S_{(162\,eV)}$ ratios with the depth of the analysis also suggests that the oxidized sulfur (168 eV) is nearer to the surface than the reduced (thiolate) sulfur (162 eV).

Concerning the surface atomic composition of the gold samples after being cleaned with ''piranha solution'' and before immersion in the thiol solutions, no sulfur and nitrogen were found by XPS (data not shown). However, as described by other authors [19, 38], there are always carbon and oxygen contaminants on the gold surface that will be displaced by the alkanethiol due to its strong affinity to gold.

3.2.2. Contact angle measurements

Table V shows the water contact angle measurements on gold and all the SAMs used. EG-terminated SAMs present a contact angle of 61° ± 0.7. This value is higher than that found by other authors, which is usually between 34° and 38° [21, 27]. However, Silver *et al.* [39] described a contact angle of 59.6° ± 2.3 for alkylsiloxane monolayers terminated with [–$(OCH_2CH)_3$–OH].

OH- and CH_3-terminated SAMs present the most hydrophilic (18°) and hydrophobic (107°) surfaces, respectively. The CB-terminated SAM has a moderate hydrophilicity.

The presence of CB-thiol on mixed monolayers decreases the contact angle of the EG and CH_3-terminated SAMs and increases the contact angle of the OH-terminated SAMs. These changes of the water contact angle also suggest the incorporation of CB-thiol in the monolayers.

TABLE V Water contact angle of gold and all the SAMs using the sessile drop method

SAMs	Contact angle (°)
CB	50 ± 1.0
EG	61 ± 0.7
EG–CB	51 ± 0.6
OH	18 ± 1.2
OH–CB	35 ± 0.8
CH_3	107 ± 1.3
CH_3–CB	103 ± 0.6
Au	63 ± 2.6

Gold surfaces have a water contact angle of 63 ± 2.6°. This value is similar to that found by other authors [19, 27]. Although a clean gold surface has been referred as being very hydrophilic, $\theta_a \sim 0°$ [40], after some minutes of air exposure, the contact angle of a water drop on gold rapidly increases to 30°–70° [19].

3.3. Protein adsorption

3.3.1. Quantification of HSA adsorption on different SAMs

Fig. 5 shows the HSA adsorption obtained using ^{125}I-labeled HSA on the different pure and mixed SAMs. Pure CB-, OH- and EG-terminated SAMs and mixed EG–CB and OH–CB-terminated SAMs presented low HSA adsorption (0.4–0.6 mg/m^2). Gold and hydrophobic monolayers (pure CH_3 and mixed CH_3–CB-terminated SAMs) present high HSA adsorption (2.4 mg/m^2 on gold, 1.9 mg/m^2 on pure CH_3-terminated SAMs and 2.2 mg/m^2 on CH_3– CB mixed SAMs).

The surface concentration of HSA on CH_3-terminated SAMs was similar to the ~2 mg/m^2 found by Sigal *et al.* [21] and higher than the ~0.31 mg/m^2 obtained by Tidwell *et al.* [41] for BSA. The surface concentration of HSA on OH-terminated SAMs was similar to the values found by other authors [21, 42]. Albumin adsorption to EG-terminated SAMs was higher than the almost zero found elsewhere [21–24, 41], which may be related to the higher water contact angle found on EG-terminated SAM.

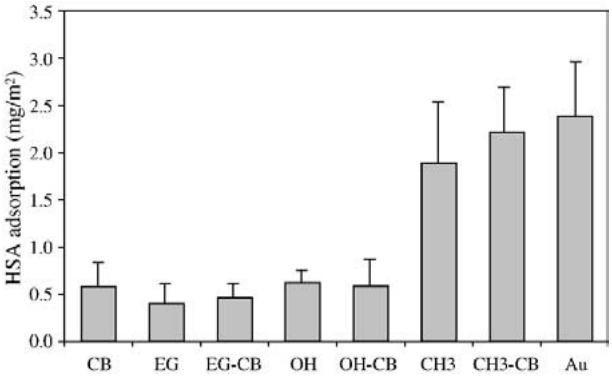

Figure 5 Human serum albumin (HSA) adsorption to gold and SAMs with and without Cibacron Blue F3G-A.

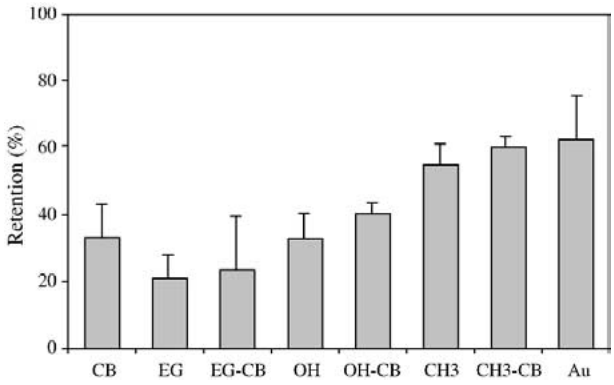

Figure 6 Percentage of ^{125}I-HSA retention to gold and SAMs with and without Cibacron Blue F3G-A, after washing over 24 h with an unlabeled albumin solution.

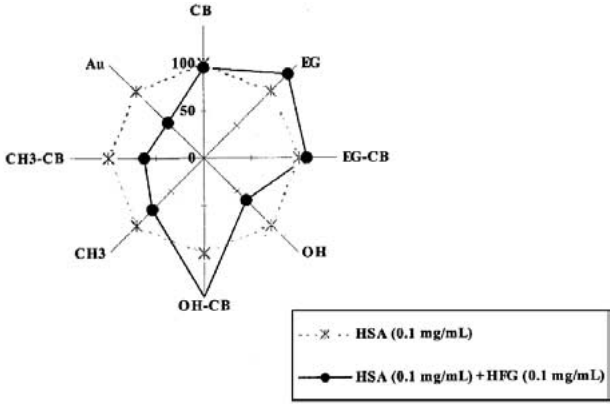

Figure 7 Competitive adsorption of HSA (0.1 mg/ml) with HFG (0.1 mg/ml) to gold and SAMs with and without Cibacron Blue F3G-A. Calculations were performed considering as 100% adsorption, the concentration of the adsorbed HSA obtained from a pure albumin solution.

3.3.2. Exchangeability of protein adsorption

The displaceability of adsorbed proteins to the different SAMs was evaluated by the exchange of the pre-adsorbed ^{125}I-labeled HSA by unlabeled albumin in solution.

Fig. 6 shows the percentage of HSA retention onto the different SAMs, after washing over 24 h with unlabeled HSA solution (1 mg/ml). The retention of the pre-adsorbed ^{125}I-HSA is small on SAMs with a low tendency for protein adsorption (CB; EG; OH; EG–CB and OH–CB SAMs). Gold and hydrophobic SAMs (CH_3 and CH_3–CB SAMs) present higher HSA retentions than the other SAM and the differences between them are not significant.

These values are in accordance with data presented in another paper [43], in which we observed higher HSA retention on gold and CH_3-terminated SAMs than on OH-terminated SAMs after washing with HSA.

3.3.3. Competitive adsorption of HSA and HFG

Fig. 7 shows the effect of the presence of the unlabeled HFG on the adsorption of ^{125}I-HSA onto different surfaces. The decrease in HSA adsorption due to the presence of fibrinogen is higher on the surfaces that demonstrate a higher affinity to the competitive protein (fibrinogen), namely Au, OH-, CH_3- and CH_3–CB terminated SAMs.

During the competitive adsorption tests, the concentration of ^{125}I-labeled HSA was 0.1 mg/ml and the same concentration of unlabeled HFG was added to the solution. Calculations were performed considering as 100% adsorption the concentration of HSA adsorbed from a pure ^{125}I-labeled HSA solution.

The decrease in albumin adsorption due to the presence of fibrinogen is surface dependent and is higher on gold surface followed by OH-, CH_3–CB and CH_3-terminated SAMs. In another work [43], it has also been demonstrated that albumin adsorption to OH-terminated SAMs is more affected by the presence of fibrinogen than adsorption to CH_3-terminated SAMs.

CB, EG, EG–CB and OH–CB SAMs show a low affinity to fibrinogen, since albumin adsorption does not decrease due to the presence of fibrinogen. The presence of fibrinogen even increases albumin adsorption on EG, EG–CB and OH–CB surfaces. The decrease in the fibrinogen affinity to OH–CB SAMs is related to the incorporation of the CB-thiol on this monolayer since pure OH-terminated SAMs show a high affinity to fibrinogen.

An explanation for the increase in HSA adsorption observed on EG, EG–CB and OH–CB when fibrinogen was present cannot be given at this stage. One possibility could be that the increase in total protein concentration may lead to preferential adsorption of one of them, HSA in this case. The results suggest that in a mixed HSA/HFG solution (1 : 1 ratio) HSA would have more affinity to the surface than HFG.

4. Discussion

In the present study, we used SAMs on gold as a model system to study the effect of immobilized Cibacron Blue F3G-A on the adsorption of HSA. For this study, tetra(ethylene glycol)-undecanethiol (EG-thiol) was synthesized and derivatized with Cibacron Blue F3G-A (CB-thiol). It is plausible to assume that CB-thiol was covalently immobilized by its triazine ring to the terminal hydroxyl group of the EG-thiol. It was suggested that this orientation of the molecule results in higher binding of albumin [14]. This CB-thiol was mixed with other alkanethiols to give three different model systems, as described in Fig. 2. EG and OH-thiols are used to decrease the non-specific protein adsorption and a CH_3- thiol was used as control. On OH–CB and CH_3–CB mixed SAMs, Cibacron Blue protrudes from the hydrophilic and hydrophobic background by a protein resistant spacer $-(O-CH_2-CH_2-)_4-$ to minimize non-specific effects in the experiments. Biospecific affinity of ligands is usually strongly dependent on the SAMs used as the background, on the dilution of the ligand and on the length of the flexible spacer [17, 44–46].

The purity of CB and EG-thiols were confirmed by NMR. The incorporation of the CB-thiol on the different model systems was confirmed by XPS and water contact angle measurements. It was demonstrated that XPS can

detect Cibacron Blue by the presence of a nitrogen peak and an additional sulfur peak with a binding energy centered at 168 eV. XPS results for EG-, OH- and CH_3-terminated SAMs are similar to those described by other authors [19, 37]. Except for the EG-terminated SAMs, that have a water contact angle higher than expected [21, 27], OH- and CH_3-terminated SAMs have water contact angles similar to those reported in the literature [21, 37]. The EG-terminated SAM may be packed imperfectly on the surface accounting for the XPS data, the contact angle and the high protein adsorption results.

Concerning SAMs preparation, XPS also demonstrated that the surface concentration of binary SAMs is not equal to the composition of the thiol solutions. Cibacron Blue was only detected on SAMs prepared from ethanolic solutions with more than 80% CB-thiol. This shows a strong preference for adsorption of *n*-alkyl thiol without Cibacron Blue head groups. This preference for the non-CB-thiol was highest on mixed monolayers prepared from CB- and CH_3- thiols. These show a low CB-thiol incorporation. The relative size of the molecules is most likely responsible for this effect; CB head groups would render the packing process more difficult.

Our data demonstrated that the Cibacron Blue molecule was exposed on the surface of the monolayer. There was much evidence supporting this. The presence of a sulfur peak centered at the binding energy of 162 eV in all the SAMs, that is characteristic of the thiolate species [28], indicates that the CB-thiol is bound to the gold surface by its thiol termination. Angle-dependent XPS data suggest that CB-thiol is oriented in such a way that Cibacron Blue is present on the top of the monolayer. Binding of Cibacron Blue to the gold surface by its sulfonic groups is not likely because oxidized sulfur species, if they adsorb to the surface at all, they do it only weakly and have a tendency to be easily displaced by other thiols in solution [36]. Lin *et al*. [29] prepared SAMs using a SO_3H-terminated thiol and demonstrated that the $-SO_3^-$ terminal group was situated at the outermost surface of the SAM. However, for pure CB-terminated SAMs the monolayer is probably disordered because of steric crowding associated with the large Cibacron Blue head group.

Regarding protein adsorption, CB, OH, EG, EG–CB and OH–CB SAMs present similar and low HSA adsorption (Fig. 5). Gold and hydrophobic monolayers (CH_3 and CH_3–CB SAMs) present high HSA adsorption. These results are in accordance with several authors, who have described higher albumin adsorption on more hydrophobic surfaces [21, 43].

Although the EG-terminated SAM demonstrated low-HSA adsorption, its value is higher than that found by other authors for BSA and other plasma proteins using surface plasmon resonance spectroscopy (SPR) [21, 42]. These reports indicate almost no adsorption.

Monolayers with low protein adsorption also exhibit lower retention of labeled albumin than gold and hydrophobic monolayers (CH_3 and CH_3–CB SAMs) after washing over 24 h with an unlabeled HSA solution (Fig. 6). The loss of exchangeability of the HSA after adsorption on hydrophobic surfaces (CH_3 and CH_3–CB SAMs) is associated with conformational changes induced by the surface [47].

In competitive adsorption studies, the presence of another protein (fibrinogen) suppresses the adsorption of the protein of interest (HSA) to different extents, depending on the affinity of the protein to the surface [32, 48]. This was observed on gold and OH, CH_3 and CH_3–CB SAMs (Fig. 7). However, EG-terminated SAMs and monolayers with CB (except CH_3–CB) demonstrated an increase in HSA affinity when fibrinogen was present in solution.

The use of oligo(ethylene glycol)-alkanethiols with the same chain length as the EG–CB SAMs (Fig. 2) in mixed monolayers could explain the lower HSA adsorption and lack of exchangeability, since Cibacron Blue may not protrude above the protein-resistant background (EG-terminated SAM). The higher affinity of albumin to the surface during the competitive adsorption studies (Fig. 7) cannot be associated with the effect of Cibacron Blue, as the pure EG-terminated SAMs also demonstrates higher affinity to HSA than to HFG.

On OH–CB mixed SAMs, the ligand clearly protrudes above the surface of the monolayer by a medium length spacer (tetra(ethylene glycol)). Although there is no increase in HSA adsorption after CB-thiol incorporation on the monolayer, a higher HSA affinity can be observed in competitive adsorption studies (Fig. 7). Since pure OH-terminated SAMs showed lower HSA affinity in relation to HFG, the increase in this affinity to albumin can be attributed to the presence of the Cibacron Blue head group. However, further experimental work must be done to evaluate if this adsorption behavior can be associated with biospecific adsorption of albumin to the immobilized Cibacron Blue.

The high albumin adsorption and retention on CH_3–CB mixed SAMs is related to the non-specific adsorption to CH_3-terminated thiols used as the background [49].

These results show that the incorporation of CB-thiol in the monolayers (Fig. 2), does not increase the HSA adsorption and exchangeability on the SAMs, in relation to the pure monolayers. However, the presence of CB-thiol decreases the affinity of fibrinogen to the OH-terminated SAMs. Since OH-terminated SAMs are not 100% resistant to non-specific protein adsorption an approach to increase biospecific adsorption could be the preparation of mixed SAMs using oligo(ethylene glycol)-terminated alkanethiols with different lengths to better resist protein adsorption and ensure enhanced CB exposure on the surface. Also, the CB density on the surface was not optimized and could be important for biospecific site presentation to albumin molecules.

5. Conclusions

In this work, Cibacron Blue F3G-A was successfully immobilized onto tetra(ethylene glycol)-undecanethiol (CB-thiol). Mixed SAMs prepared from ethanolic mixtures of CB-thiol with other functionalized alkanethiols (CH_3-, OH- and tetra(ethyleneglycol)-terminated thiols) were used to study the affinity of HSA to the immobilized Cibacron Blue. EG- and OH-thiols were

used to decrease the non-specific protein adsorption and a CH_3-thiol was used as a control. On OH–CB and CH_3–CB mixed SAMs, Cibacron Blue protrudes, respectively, from the hydrophilic and hydrophobic background by a hydrophilic spacer. XPS and water contact angle measurements demonstrated the incorporation of CB-thiol on the monolayers. Results have shown that the incorporation of CB-thiol on the monolayers do not increase the HSA adsorption and exchangeability on the SAMs. This is in contrast to published works by other investigators. Although specific adsorption of HSA to the immobilized Cibacron Blue F3G-A was not demonstrated, the presence of CB-thiol decreases the affinity of fibrinogen to the OH-terminated SAMs.

Acknowledgments

The authors would like to thank Dr Paulo Freitas and Dr Susana Freitas (INESC) for gold sample preparation, and Dr Carlos Sá (CEMUP) for assistance in the XPS investigation. Mª Cristina L. Martins is grateful to UWEB (University of Washington Engineered Biomaterials) and NESAC/BIO for supporting and enabling her to carry out research work as part of her Ph.D. and to the Portuguese Foundation for Science and Technology (FCT) for awarding her a scholarship under the program PRAXIS XXI.

References

1. B. D. RATNER, *J. Mol. Recognit.* **9** (1996) 617.
2. K. KOTTKE-MARCHANT, J. M. ANDERSON, Y. UMEMURA and R. E. MARCHANT, *Biomaterials* **10** (1998) 147.
3. A. A. A. DE QUEIROZ, E. R. BARRAK, H. A. C. GIL and O. Z. HIGA, *J. Biomater. Sci. Polym. Ed.* **8** (1997) 667.
4. K. R. KAMATH and K. PARK, *J. Appl. Biomater.* **5** (1994) 163.
5. M. S. MUNRO, A. J. QUATTRONE, S. R. ELLSWORTH, P. KULKARNI and R. C. EBERHART, *Trans. Am. Soc. Artif. Intern. Organs* **27** (1981) 499.
6. J. JI, L. FENG and M. A. BARBOSA, *Biomaterials* **22** (2001) 3015.
7. J. R. KEOGH and J. W. EATON, *J. Lab. Clin. Med.* **121** (1994) 537.
8. D. WANG, B. CHEN, J. JI and L. FENG, *Bioconjugate Chem.* **13** (2002) 792.
9. J. JI, M. A. BARBOSA, L. FENG and J. SHEN, *J. Mat. Sci. Mat. Med.* **13** (2002) 677.
10. C. D. MCFARLAND, M. JENKINS, H. J. GRIESSER, R. C. CHATELIER, J. G. STEELE and P. A. UNDERWOOD, *J. Biomater. Sci. Polym. Ed.* **9** (1998) 1207.
11. C. D. MCFARLAND, C. D. FILIPPIS, M. JENKINS, A. TUNSTELL, N. P. RHODES, D. F. WILLIAMS and J. G. STEELE, *ibid.* **9** (1998) 1277.
12. G. KOPPERSCHLAGER, H. J. BOHME and E. HOFMANN, *Adv. Biochem. Eng.* **25** (1982) 101.
13. J. TRAVIS, J. BOWEN, D. TEWKSBURY, D. JOHNSON and R. PANNELL, *Biochem. J.* **157** (1976) 301.
14. R. L. LEATHERBARROW and P. D. G. DEAN, *ibid.* **189** (1980) 27.
15. M. C. L. MARTINS, D. WANG, J. JI, L. FENG and M. A. BARBOSA, *J. Biomater. Sci. Polym. Ed.* **14** (2003) 439.
16. M. DOCKAL, D. C. CARTER and F. RUKER, *J. Biol. Chem.* **274** (1999) 29303.
17. E. OSTUNI, L. YAN and G. M. WHITESIDES, *Colloid Surf. B-Biointerfaces* **15** (1999) 3.
18. A. ULMAN, ''An Introduction to Ultrathin Organic Films: From Langmuir-Blodgett to Self-Assembled'' (Academic Press Inc: San Diego, CA, USA, 1991).
19. C. D. BAIN, E. B. TROUGHTON, Y. T. TAO, J. EVALL, G. M. WHITESIDES and R. G. NUZZO, *J. Am. Chem. Soc.* **111** (1989) 321.
20. M. D. PORTER, T. B. BRIGHT, D. L. ALLARA and C. E. D. CHIDSEY, *ibid.* **109** (1987) 3559.
21. G. B. SIGAL, M. MRKSICH and G. M. WHITESIDES, *ibid.* **120** (1998) 3464.
22. R. R. SEIGAL, P. HARDER, R. DAHINT and M. GRUNZE, *Anal. Chem.* **69** (1997) 3321.
23. G. P. LÓPEZ, H. A. BIEBUYCK, R. HARTER, A. KUMAR and G. M. WHITESIDES, *J. Am. Chem. Soc.* **115** (1993) 10774.
24. K. PRIME and G. M. WHITESIDES, *Science* **252** (1991) 1164.
25. J. A. CHINN, T. A. HORBETT and B. D. RATNER, *Thromb. Haemost.* **65** (1991) 608.
26. V. GEHANNO, P. P. FREITAS, A. VELOSO, J. FERREIRA, B. ALMEIDA, J. B. SOUSA, A. KLING, J. C. SOARES and M. F. SILVA, *IEEE Trans. Magn.* **35** (1999) 4361.
27. C. PALE-GROSDEMANGE, E. S. SIMON, K. L. PRIME and G. M. WHITESIDES, *J. Am. Chem. Soc.* **113** (1991) 12.
28. D. G. CASTNER, K. HINDS and D. W. GRAINGER, *Langmuir* **12** (1996) 5083.
29. J. C. LIN and W. H. CHUANG, *J. Biomed. Mater. Res.* **51** (2000) 413.
30. J. LIMA, S. R. SOUSA, A. FERREIRA and M. A. BARBOSA, *ibid.* **55** (2001) 45.
31. ''Iodine-125, a Guide to Radioiodination Techniques – Amersham Life Science'' (Amersham International plc, Amersham Place, Little Chalfont, Bucks. HP7 9NA, England, 1993) p. 64.
32. T. A. HORBETT, Techniques for protein adsorption studies, in ''Techniques of Biocompatibility Tests'', edited by D. F. Williams (Harcover, CRC Pr, 1986) p. 183.
33. Y. J. DU, R. M. CORNELIUS and J. L. BRASH, *Colloid Surf. B-Biointerfaces* **17** (2000) 59.
34. G. BEAMSON and D. BRIGGS, ''High Resolution XPS of Organic Polymers – The Scienta ESCA300 Database'' (John Wiley & Sons Ltd, Chichester, England, 1992).
35. htpp://www.lasurface.com/.
36. M. J. TARLOV, D. R. F. BURGESS, JR and G. GILLEN, *J. Am. Chem. Soc.* **115** (1993) 5305.
37. V. A. TEGOULIA and S. L. COOPER, *J. Biom. Mater. Res.* **50** (2000) 291.
38. T. ISHIDA, S. TSUNEDA, N. NISHIDA, M. HARA, H. SASABE and W. KNOLL, *Langmuir* **13** (1997) 4638.
39. J. H. SILVER, R. W. HERGENROTHER, J. C. LIN, F. LIM, H. B. LIN, T. OKADA, M. K. CHAUDHURY and S. L. COOPER, *J. Biom. Mater. Res.* **29** (1995) 535.
40. T. SMITH, *J. Colloid. Interf. Sci.* **75** (1980) 51.
41. C. D. TIDWELL, S. I. ERTEL and B. D. RATNER, *Langmuir* **13** (1997) 3404.
42. V. SILIN, H. WEETALL and D. VANDERAH, *J. Colloid. Interf. Sci.* **185** (1997) 94.
43. M. C. L. MARTINS, B. D. RATNER and M. A. BARBOSA, *J. Biom. Mater. Res.* **67A** (2003) 158.
44. D. D. SCHLERETH, *Sens. Actuator B-Chem.* **43** (1997) 78.
45. M. MRKSICH, J. R. GRUNWELL and G. M. WHITESIDES, *J. Am. Chem. Soc.* **117** (1995) 12009.
46. C. D. HODNELAND, Y. S. LEE, D. H. MIN and M. MRKSICH, *PNAS* **99** (2002) 5048.
47. M. MALMSTEN and B. LASSEN, *J. Colloid. Interf. Sci.* **166** (1994) 490.
48. L. FENG and J. D. ANDRADE, *Biomaterials* **15** (1994) 323.
49. L. BERTILSSON, H. J. BUTT, G. NELLES and D. D. SCHLERETH, *Biosens. Bioelectron.* **12** (1997) 839.

Received 7 March
and accepted 3 June 2003